First Principles Study on Hydrogen Desorption from a Metal (=Al, Ti, Mn, Ni) Doped MgH2 (110) Surface

ARTICLE *in* THE JOURNAL OF PHYSICAL CHEMISTRY C · JUNE 2010

Impact Factor: 4.77 · DOI: 10.1021/jp103066g

3 AUTHORS, INCLUDING:

Yan Song
Harbin Institute of Technology
83 PUBLICATIONS **1,259** CITATIONS
SEE PROFILE

Rado Yang
ASM International N.V.
247 PUBLICATIONS **3,971** CITATIONS
SEE PROFILE

First Principles Study on Hydrogen Desorption from a Metal (=Al, Ti, Mn, Ni) Doped MgH_2 (110) Surface

J. H. Dai,[†] Y. Song,*[,†] and R. Yang[‡]

School of Materials Science and Engineering, Harbin Institute of Technology at Weihai, 2 West Wenhua Road, Weihai 264209, China, Institute of Metal Research, Chinese Academy of Sciences, 72 Wenhua Road, Shenyang 110016, China

Received: April 5, 2010; Revised Manuscript Received: May 19, 2010

First principles calculations on an Al, Ti, Mn, and Ni doped MgH_2 (110) surface were carried out to study the influence of dopants on the dehydrogenation properties of MgH_2. It was shown that Al prefers to substitute for an Mg atom, whereas Ti, Mn, and Ni prefer to occupy interstitial sites. The dopants used different mechanisms to improve the dehydrogenation properties of MgH_2. Al weakens the interactions between the Mg and the H atoms in its vicinity and so slightly improved the dehydrogenation properties of the Al doped system. The H atoms near the dopants of the transition metal doped systems were dramatically distorted. Ti has a high potential to generate a TiH_2 phase by attracting two H atoms, which frees one H atom from its host Mg atom. The dehydrogenation properties of the Mn doped system were improved by the formation of a Mn−H cluster with a similar structure to Mg_3MnH_7 but weaker interactions between its atoms. If the MgH_2 (110) surface is doped with Ni, the Ni will attract four H atoms to form a regular tetrahedral NiH_4 group almost identical in structure to that in Mg_2NiH_4. The improvement of the dehydrogenation properties of Ni-doped MgH_2 is expected as the bonding between the Mg and the H atoms is weakened, and there is a high possibility that the Mg_2NiH_4 phase will be formed, which is thermodynamically less stable than the MgH_2 in this system.

1. Introduction

Hydrogen, with its excellent electrochemical reactivity, reasonable power density, and zero emission characteristics when used in pure form in fuel cells, is an attractive pollution-free clean energy carrier. A variety of metal hydrides could be used as a hydrogen storage medium. Magnesium hydride is one of the most promising candidates; it has been investigated extensively over the past few decades as it is lightweight and cheap and has a high hydrogen capacity of 7.6 wt %. However, its poor thermodynamic and kinetic properties greatly limit its practical applications.[1,2]

Many studies have been carried out to investigate the adsorption and desorption kinetics of MgH_2. Alloying MgH_2 with transition metals and transition metal oxides improves its H_2 sorption kinetics and its thermodynamic properties.[3−10] In 1993, Bogdanović et al.[2,11] made a detailed comparison of the thermochemical and hydrogen storage properties of Mg-MgH_2 materials in Ni-doped and undoped systems. They found that the Ni dopant can significantly improve the cyclical stability and increase the rate of hydrogenation and dehydrogenation. Bobet et al.[12] reported that Mg's ability to store hydrogen could be enhanced by reactive mechanical alloying it with 10 wt % Co, Ni, or Fe. Gutfleish et al. have also found alloying Mg with Ni (1 wt %) and Pd (2 wt %) achieves excellent hydrogen absorption and desorption kinetics and cyclical stability.[13] Song et al.[9] and Shang et al.[10] have found that Ni is a better alloying element than Ti as the heat of formation of a MgH_2−Ni system is −44.97 kJ/molH_2, higher than that of a MgH_2−Ti system. In contrast, Liang et al. found that V and Ti catalyze hydrogen absorption and desorption in MgH_2 better than Ni, and that MgH_2−V and MgH_2−Ti systems show faster absorption and desorption kinetics than the other 3d elements they investigated.[3] Jensen et al.[14] used in situ time-resolved powder X-ray diffraction to study the influence of a Ni dopant on the dehydrogenation properties of a surface-oxided magnesium hydride. They showed that the dehydrogenation kinetics were highly influenced by the air surrounding the hydride, and the Ni dopant decreased the dehydrogenation barrier and catalyzed the recombination of H to H_2.[14] More recently, Lu et al.[15] investigated the desorption capacity, thermodynamics and kinetics of Ti- and Ni/Ti-catalyzed Mg hydrides, and found that the Ti and Ni/Ti catalysts improved the thermodynamic and kinetic properties of MgH_2 and that a Ni:Ti ratio of 4:1 gave the highest rate of hydrogen desorption. Zaluska et al.[16] studied the kinetics of hydrogen absorption and desorption of Li, Al, Ti, V, Mn, Zr, and Y doped nanocrystalline magnesium hydrides, and found that the lowest temperatures at which hydrogen adsorption occurred were in the systems using V + Zr and Mn + Zr Mg alloys. Recently, Lu et al.[17] have demonstrated that a nanostructured uniform mixture of MgH_2−0.1TiH_2 powder has much better kinetics of dehydrogenation and hydrogenation than commercial MgH_2.

Larsson et al.[18] carried out first principles calculations based on DFT to show that Ti, V, Fe, and Ni significantly lowered the H_2 desorption energy of MgH_2 nanoclusters. Computational studies by Liang[19] and Song et al.[20] used density functional theory to show that substituting the two Mg atoms of MgH_2 with a Li and an Al atom[19] or by a Ti and a Ni atom[20] can improve its hydrogen storage processes by lowering the reaction and activation energies and by weakening the Mg−H bonds. More recently, Pozzo and Alfè[21] investigated the dissociation and diffusion of hydrogen onto a transition metal doped Mg (0001) surface. They found that the transition metals on the

* To whom correspondence should be addressed. E-mail: sy@hitwh.edu.cn.
† Harbin Institute of Technology.
‡ Chinese Academy of Sciences.

10.1021/jp103066g
Published on Web 06/03/2010

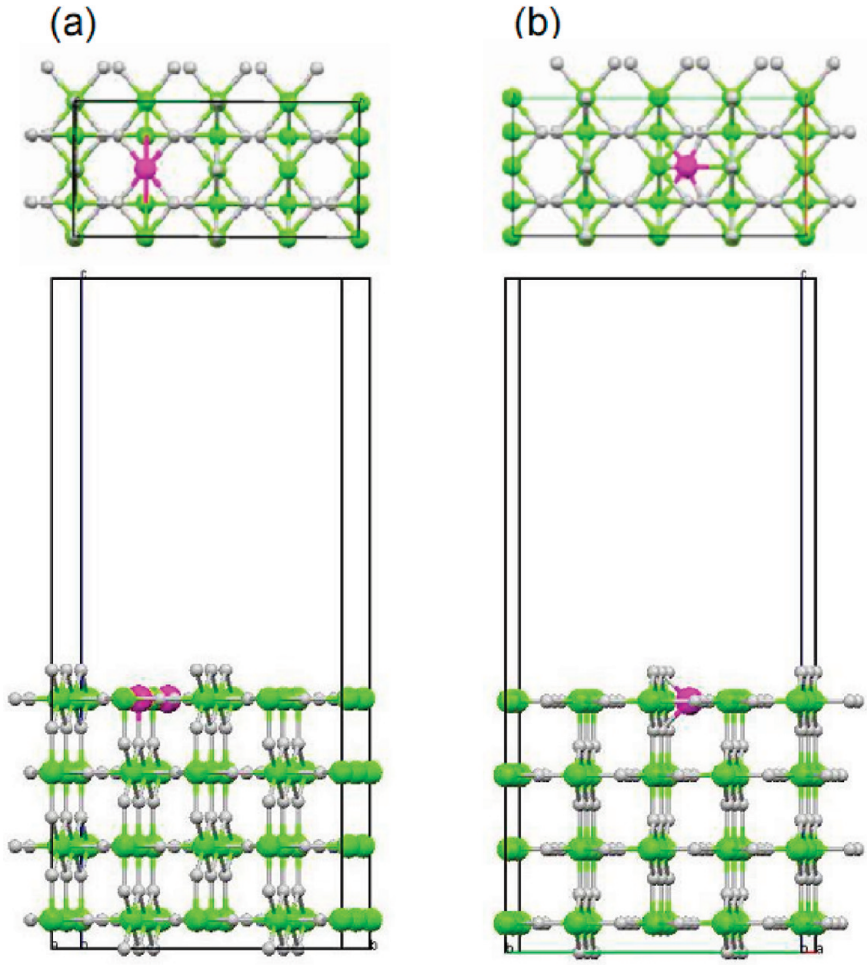

Figure 1. Supercells employed in the present work: (a) the top and side views of the substitution and (b) the top and side views of the interstitial occupation. The light gray, green and magenta balls denote the H, the Mg, and the dopant, respectively.

left-hand side of the periodic table will lower the hydrogen dissociation barrier but the strong bonding between the dissociated H atoms and the metal dopant will slow the absorption process as it deactivates the catalyst. The transition metals on the right-hand side of the periodic table do not bind too strongly to the H atoms but only have a limited effect on the dissociation barrier.[21] Kelkar and Pal[22] investigated the influence of Al and Si dopants on the thermodynamics and kinetics of MgH_2. Their results showed that the reduction of the band gap between the valence and the conduction bands reduced the stability of doped MgH_2. However, doping the MgH_2 with Al or Si does not affect the activation energy barriers for H_2 desorption from its (001) surface.[22] Li et al. carried out an ab initio molecular dynamics simulation to investigate the influence of Nb and Mg vacancies on the dehydrogenation properties of MgH_2.[23] They reported that Nb dopants decrease the dehydrogenation barrier of MgH_2 so that hydrogen molecules are formed at a temperature of 300 K after 200 fs.[23] Du et al. studied the low index magnesium hydride surfaces (001) and (110), and found that the surface energy of the (110) surface is about 0.013 eV/Å^2 lower than that of the (001) surface.[24]

It is desirable to understand the effects dopants have on the hydrogenation/dehydrogenation properties of MgH_2. In this study, we will investigate the geometric and electronic structures of a doped MgH_2 (110) surface as it is more stable than the (001) surface.[24] First principles total energy calculations were used to study the dopant's site preferences and its influence on the dehydrogenation properties of the MgH_2.

2. Methodology

The electronic structure and total energy of M (M = Al, Ti, Mn, or Ni) doped MgH_2 systems were calculated by VASP code using the generalized gradient approximation of Perdew and Wang.[25−27] The project augmented wave method was used to span out the valence electron density.[28] A cutoff energy of 450 eV and a Gaussian smearing method with an energy broadening of 0.2 eV were used throughout. Electronic structures were considered self-consistent if two consecutive energies and forces differed by less than 0.01 meV and 0.01 eV/Å. The surface of MgH_2 was simulated by a 2 × 2 slab model in both the *a* and *b* directions. The accuracy of the total energy on the *k*-mesh and the cutoff energy was calculated for several *k*-meshes, and as a result this work uses a 3 × 3 × 1 *k*-mesh.

3. Results and Discussions

3.1. Occupation Energy and Location Preference. MgH_2 has tetragonal symmetry ($P4_2/mnm$, group no. 136). The Mg atom occupies the 2*a* (0, 0, 0) site and the H atom occupies the 4f (0.304, 0.304, 0) site. The lattice parameters are $a = 0.4501$ nm and $c = 0.301$ nm.[29] A full relaxation of a unit cell of MgH_2 was performed and the resulting lattice parameters of $a = 0.4497$ nm and $c = 0.3003$ nm were very close to the experimental values.[29]

The surface supercell was built from a 2 × 2 slab model that consisted of eight atomic layers separated by a 1.7 nm vacuum and contained a total of 96 atoms for the undoped MgH_2 system.

TABLE 1: Coordinates and Occupation Energy, E_{occ}, of Dopants in (110) Surface after Geometric Relaxation and the Dehydrogenation Energy, E_d, from the M (=Al, Ti, Mn, and Ni) Doped MgH_2 (110) Surface[a]

	coordinates				
M	*u*	*v*	*w*	E_{occ} (eV)	E_d (eV)
MgH_2					1.915
Al (subs)	0.5	0.2500	0.3666	1.732	1.923
(int)	0.5	0.3469	0.4010	2.159	1.984
Ti (subs)	0.5	0.2500	0.3663	1.605	1.691
(int)	0.5	0.3819	0.3240	1.185	1.608
Mn (subs)	0.5	0.2500	0.3632	2.678	1.342
(int)	0.5	0.3527	0.3436	1.896	1.509
Ni (subs)	0.5	0.2500	0.3598	1.589	1.295
(int)	0.5	0.4035	0.3765	0.760	1.815

[a] The initial coordinates of dopant M are (0.5, 0.25, 0.3725) for substitution, M(subs), and (0.5, 0.4030, 0.3725) for interstitial occupation, M(int), respectively, in the considered $(Mg_{32-x}M_{x+y})H_{64}$ system.

The M-doped system is denoted as $(Mg_{32-x}M_{x+y})H_{64}$, where ($x = 1$, $y = 0$) means a M atom has been substituted for a Mg atom on the surface and ($x = 0$, $y = 1$) means that the M atom occupies an interstitial site in the surface. The initial coordinates of the dopant M are (0.5, 0.25, 0.3725) for a substitution and (0.5, 0.4030, 0.3725) for an interstitial occupation as shown in Figure 1.

The three topmost layers were allowed to relax, while the rest were kept at the bulk interatomic distances. The convergences of the surface energy on the thickness of the slab and the space of the vacuum of the supercell were checked using a threshold of 1 meV/Å^2. The estimated surface energy was 0.0358 eV/Å^2. The H atoms in the top layer of the undoped MgH_2 (110) surface moved about 0.020 nm outward and their corresponding Mg atoms moved about 0.018 nm inward. Similar movements were observed by Du et al.[24]

To identify which site the dopant M prefers we define the occupation energy in eq 1, which uses E(X) for the total energy of system X

$$E_{occ} = E(Mg_{32-x}M_{x+y}H_{64}) - [E(Mg_{32}H_{64}) + (x + y)E(M) - xE(Mg)] \quad (1)$$

Table 1 lists the estimated coordinates of dopants and the occupation energy of each system. In the Al-doped system, the Al atom usually substitutes for an Mg atom with an occupation energy of 1.73 eV, and moves to a distance of 0.083 nm above the surface (where it would have an occupation energy of 2.16 eV if it occupied an interstitial site). The transition metals considered here (Ti, Mn, and Ni) are the least likely to substitute for the Mg atom due to the high occupation energies required. Instead, they prefer to occupy the interstitial sites whose occupation energies are lower than those of the substitution occupations. The analysis in the following sections therefore only covers the electronic structures and bonding characteristics of the Al substitution, denoted below as Al(subs), and the Ti, Mn, and Ni interstitial occupation, denoted as M(int). Substituting the parameters $x = 1$, $y = 0$ and $x = 0$, $y = 1$ into eq 1 gives the occupation energy of the Al substitution and the Ti, Mn, and Ni interstitial occupation, respectively.

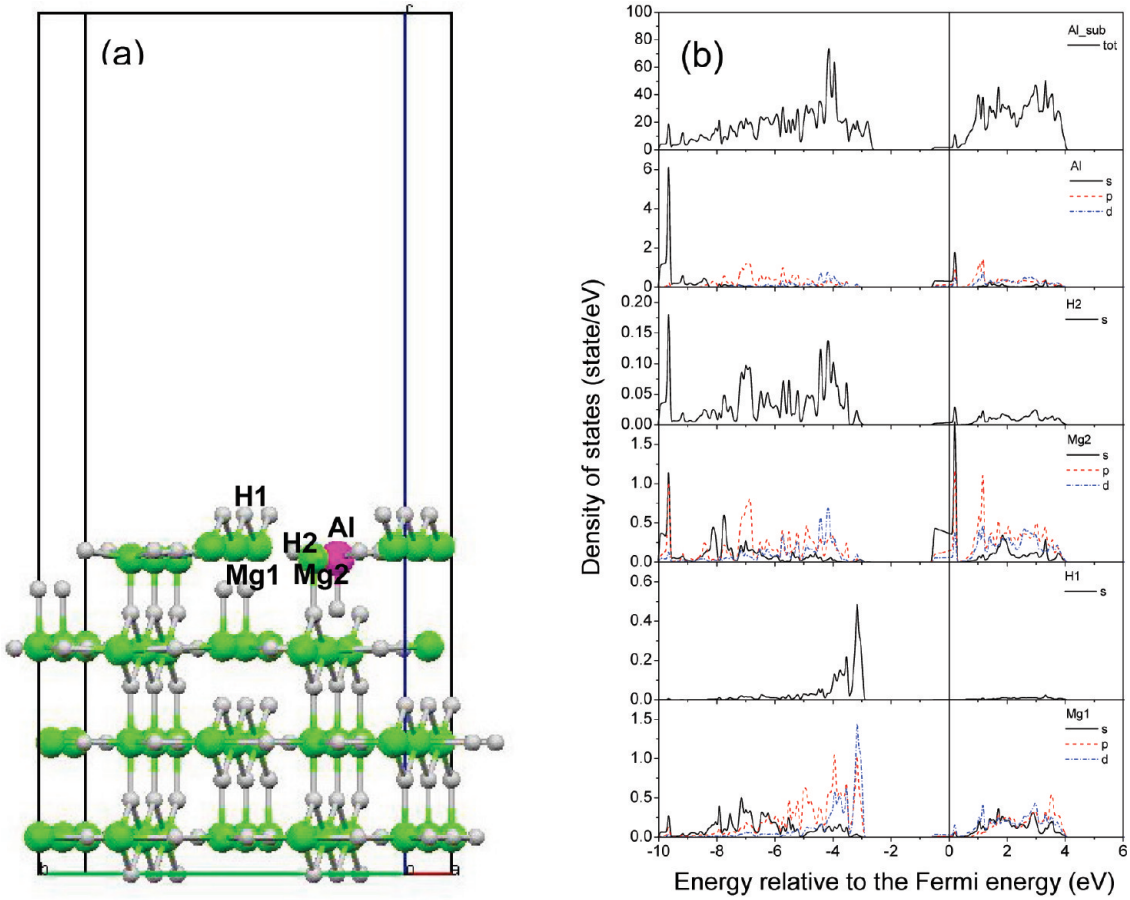

Figure 2. Substitution of Al for an Mg atom in the (110) surface of MgH_2. (a) The final structure and (b) the total and partial density of states.

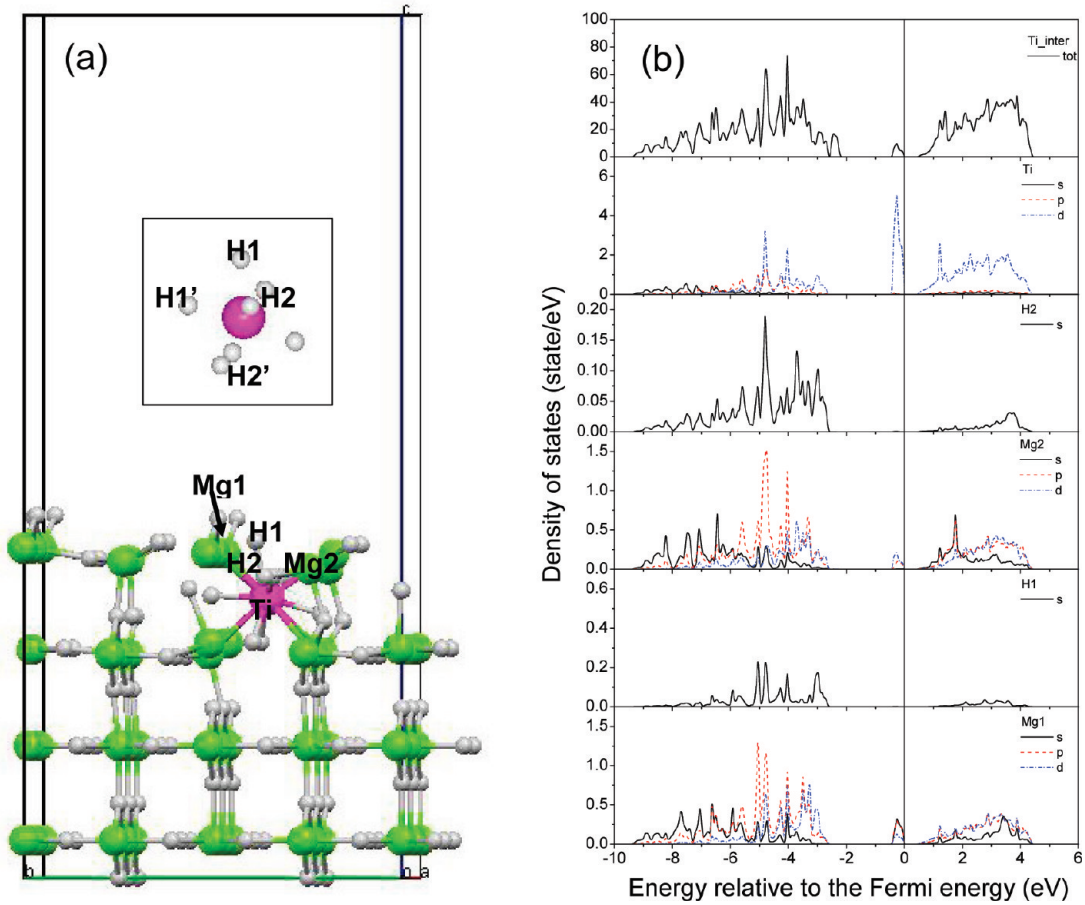

Figure 3. Interstitial occupation of Ti in the (110) surface of MgH_2. (a) The final structure and (b) the total and partial density of states. Insert is the Ti−H group, where H1′ and H2′ are symmetrically equivalent to the H1 and H2 atoms, respectively.

3.2. Electronic Structures and Bonding Interactions. The electronic structure of the Al substitution system was plotted in Figure 2. Figure 2a shows the geometry of this system after relaxation. The Al dopant is located near the host Mg atom, surrounded by H atoms (labeled H2) at a distance of 0.1784 nm. The Al−H2 bond is about 0.017 nm shorter than the original Mg−H2 bond, and the Mg2−H2 bond was stretched from 0.1955 to 0.2015 nm. The Mg1−H1 bond is compressed by 0.01 to 0.1855 nm, which implies that the Mg1−H1 bond has now been strengthened. Figure 2b is the density of states (DOSs) for this system. The doping has moved the bottom of the conduction band (CB) below the Fermi energy. It is therefore reasonable to expect that the Mg−H bonds, especially the Mg2−H2 bonds, are easier to break in this system than in its undoped counterpart. Similar behavior was observed in the Al bulk doped MgH_2.[9,22] The bonding states are distributed throughout the energy range from −10 to −2.5 eV below the Fermi energy. There is a *sp* hybridization between the Mg1 and the H1 atoms at −3.0 eV. The bonding peaks of the Mg2 p and H2 s electrons in the energy range from −5.0 to −3.0 eV contribute to the valence bond in the total DOS at the same energy range. The Mg2 p electrons distributed around −7.0 eV interact with both the H2 s and Al p electrons as the three atoms all have narrow peaks in same energy range. The Al atom is more likely to interact weakly with its surrounding Mg atoms (the Mg2 atoms) than with the H atoms, and is more likely to weaken the Mg2−H2 bonds in the surface than weaken the Mg1−H1 bonds above it.

Figure 3 shows the final structure and density of states of the Ti interstitially doped system. Figure 3a shows Ti atom moving about 0.14 nm inward from its initial position, greatly distorting its surrounding H atoms (particularly the H1 and H2 atoms) and moving them away from their initial positions. The distances between the Mg and H atoms changed dramatically; the bond lengths of the Mg1−H1 and the Mg2−H2 bonds grew 4% and 36% to 0.2034 and 0.2651 nm from the original Mg−H bond length of 0.1955 nm. The distances between the Ti and H1 atoms and the Ti and H2 atoms are 0.1952 and 0.1889 nm, respectively. Figure 3a shows that the H1 and H2 atoms moved about 0.074 and 0.069 nm in the *c* direction after the Ti atom. The Ti atom probably captures two H2 atoms and frees an H1 atom from the Mg1 atom as observed in Ti-doped $NaAlH_4$ and $LiAlH_4$ systems.[30,31]

Figure 3b shows the total and partial DOSs of this system. The isolated bonding peak just below the Fermi energy in the total DOS is caused by the Ti d states and small contributions from the Mg1 s and Mg2 p states. Unlike the Ti bulk doped MgH_2 system, the gap between the valence and conduction bands is reduced to about 0.5 eV.[8,9,32,33] The partial DOSs show that there is a greater interaction between the Mg2 and H2 atoms than in undoped MgH_2, whereas the reduction in the magnitude of the sp hybridization peaks between the Mg1 and H1 atoms in the valence band weakened their interactions. The Ti's pull on the H1 atom could be due to the small overlap of the peaks of the Ti d orbitals at −4.0 and −3.0 eV and the H1 s orbital at the same energies. Figure 3b also shows that there is an overlap between the Ti d, the H2 s and the Mg1 p states at −4.8 eV below the Fermi energy. This, coupled with the above geometry analysis, means we can expect a bonding interaction between the Ti and H2 atoms.

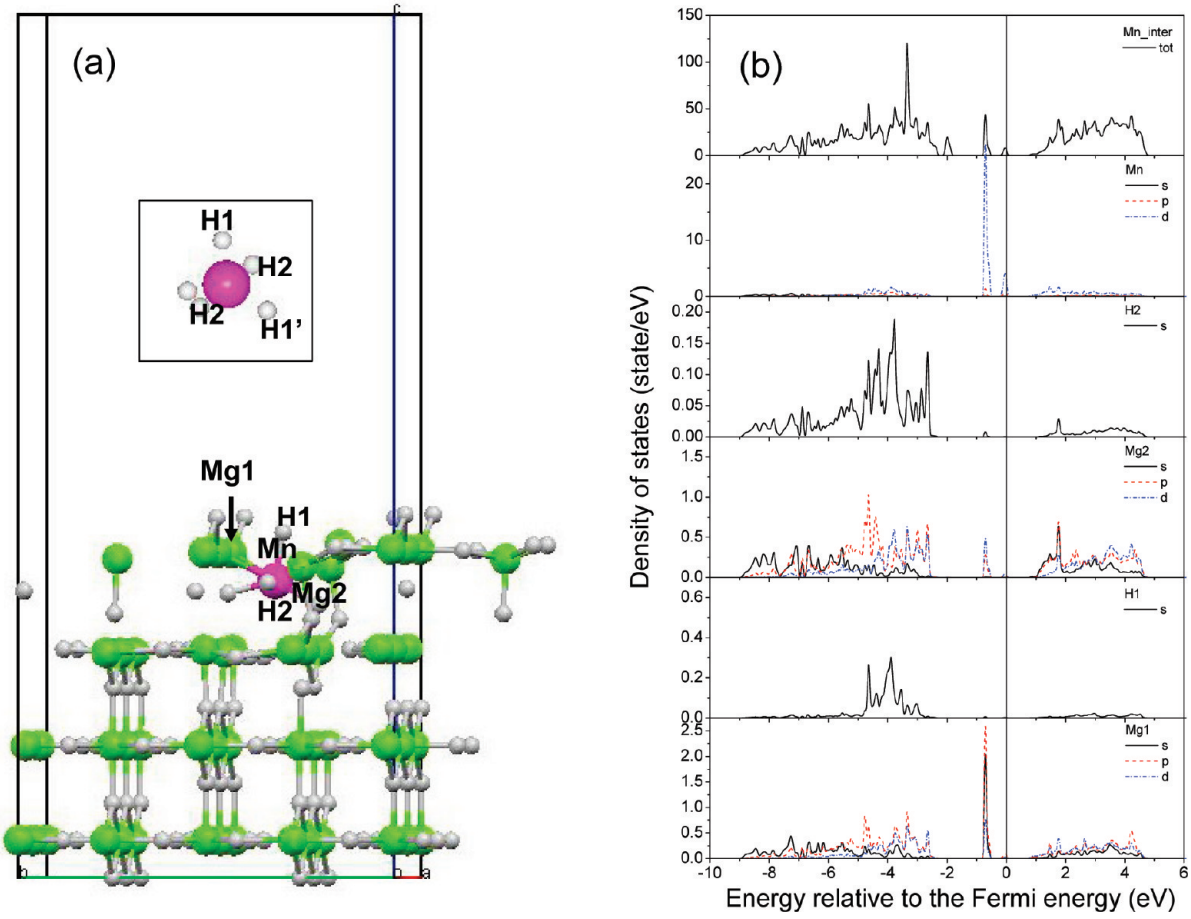

Figure 4. Interstitial occupation of Mn in the (110) surface of MgH_2. (a) The final structure and (b) the total and partial density of states. The insert shows the Mn−H group, where H1′ is symmetrically equivalent to the H1 atom.

In the Mn doped system (Figure 4), the Mn starts at the center of a triangle of three surface Mg atoms (the Mg1 atoms). A full relaxation expands the triangle and moves the Mn out of the triangle plane and toward the MgH_2, to a point 0.08 nm from surface. The H1 atom is freed from its host Mg1 atom (they finish with a distance of 0.2642 nm between them) and is moved toward to the Mn. Although the H2 atoms moved all the way from (0.25, 0.3480, 0.3725) to (0.2236, 0.3524, 0.3415) the Mg2−H2 bond length barely changed. The other two H atoms (labeled H1′) in Figure 4a are symmetrically equivalent to the H1 atom in the bulk MgH_2. The H1′−Mg bonds are stretched to 0.1987 nm from 0.1955 nm in the undoped system. The insert in Figure 4a shows that the Mn's final position is surrounded by five H atoms at distances of about 0.1650 nm. Two of the H1′ atoms in this insert are trapped in the MgH_2 and so are only moved a short distance away from their initial positions. This only slightly increases the length of the H1′−Mg bond, implying that these atoms are weakly affected by the Mn. The remaining H1 and H2 atoms were moved to leave 0.1650 nm between the Mn and the H1 atom, 0.1665 nm between the Mn and the two H2 atoms and a H1−Mn−H2 angle of 92.04°. The geometric structure of this Mn−H cluster is similar to that in the Mg_3MnH_7 compound, where the bond length of the Mn−H bond is 0.1633 nm and the H−Mn−H angle is 90°.[34]

Figure 4b is the total and partial DOSs of this system. The addition of Mn causes hybridization between the Mn and the host Mg atoms that results in a new peak at −0.8 eV below the Fermi energy in the total DOS. The peaks of the partial DOS of the H1 are contained in the energy region from −5.0 to −2.5 eV below the Fermi energy. The addition of the Mn has dramatically reduced the interactions between the H1 and Mg1 atoms as it attracts the Mg1 p electrons (the peak of the Mg1′s partial DOS at −0.8 eV), lowers the amplitude of the Mg1′s partial DOSs in the energy region below −2.5 eV, and confines the H1′s bonding states. However, the Mn only weakly influences the interactions between the H2 and Mg2 atoms as there are no significant changes in the distributions of their partial DOSs. The Mn is unlikely to form bonds with the five H atoms surrounding it as the Mn d electrons are strictly localized around −0.8 eV below the Fermi energy where there are no peaks belonging to H atoms. This means that there are no interactions between the Mn and H atoms, and so the dehydrogenation properties of Mn-doped MgH_2 are improved.

The geometric structure and the DOSs of the Ni-doped system are shown in Figure 5. Figure 5a shows that the Ni atom has only moved 0.01 nm toward to the vacuum after the geometry relaxation, which in turn has caused its neighboring Mg atoms and two H2 atoms to move slightly outward. The Ni pushed away its neighboring Mg atoms, but pulled forward one H1, one H1′ and two H2 atoms. The Ni−H distances are 0.1645, 0.1614, and 0.1592 nm for the H1, H1′, and H2 atoms, respectively. The insert in Figure 5a shows the nearly regular tetrahedral configuration formed around the Ni atom by these four H atoms. It is interesting to note that the Ni atom in Mg_2NiH_4 is also surrounded by a tetrahedral structure with an H atom in each corner, Ni−H bond lengths in the range from 0.152 to 0.157 nm and H−Ni−H angles between 103 and 119°. The Ni doped MgH_2 (110) surface therefore has a higher probability of forming a Ni−H tetrahedral cluster that acts as a seed to form Mg_2NiH_4 phase. The Ni doped MgH_2 is dehydrogenated in two stages; the H atoms are

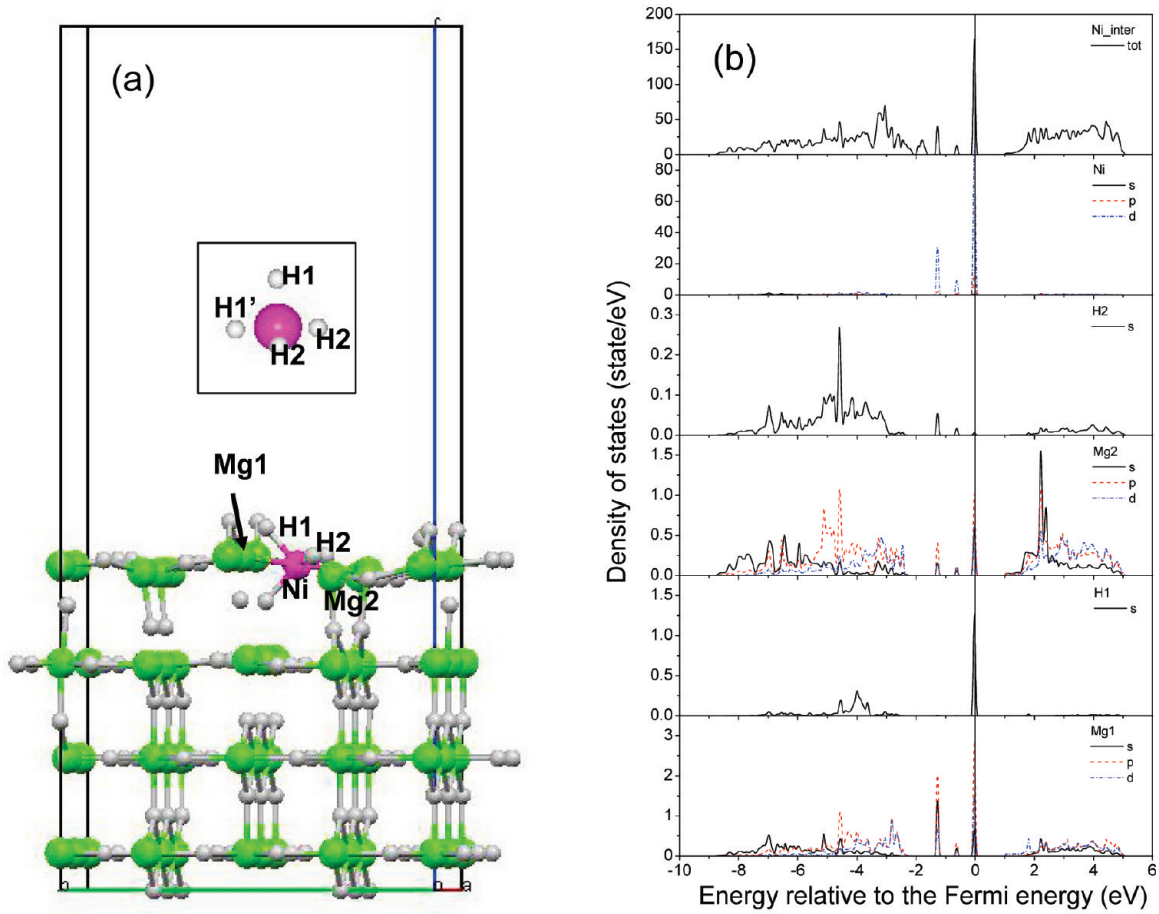

Figure 5. Interstitial occupation of Ni in the (110) surface of MgH_2. (a) The final structure and (b) the total and partial density of states. The insert shows the Ni−H group, where H1′ is symmetrically equivalent to the H1 atom.

first attracted by the dopant Ni to form a NiH_4 group and therefore the Mg_2NiH_4 phase, and then the H atoms are released by the distortion of the NiH_4 group. Doping the MgH_2 with Ni improves its dehydrogenation properties as the Mg_2NiH_4 phase is less stable than MgH_2 phase.

The total and partial DOSs of the Ni-doped system are illustrated in Figure 5b. The partial DOSs of Ni d states appear at −1.4 eV, −0.6 eV, and the Fermi energy. The partial DOSs of Mg1 p and Mg2 p electrons are dramatically changed when a Ni dopant is used. Three peaks that overlap slightly with the partial DOSs of the Ni d electrons were induced and the magnitude of the remaining bonding peaks of the Mg atoms between −8.0 and −2.3 eV was reduced. These characteristics indicate that there are interactions between the Mg and Ni atoms, which could induce a new phase such as Mg_2NiH_4. This behavior is similar to that of the Mn doped system, but the Ni doped system induced two more bonding peaks of Mg p (Mg1 or Mg2) electrons than it did (Figure 4b). The partial DOSs of the H atoms show the difference between the two systems. The partial DOSs of H1 s electrons in the energy range between −5.0 and −3.5 eV were lower than those in the Mn doped system, and a high peak at the Fermi energy was induced in the Ni doped system. The partial DOSs of H2 s electrons are highly localized in the Ni doped system; there is one main bonding peak at −4.7 eV and two new smaller peaks at −1.4 and −0.6 eV, all of which overlap the Ni d electrons in the same energy area (Figure 5b). It is therefore likely these overlaps in the energy range from −1.4 eV to the Fermi energy will cause the Ni atom to form chemical bonds with its surrounding H atoms, producing a Ni−H group as discussed above.

The above geometric and electronic structural characteristics of the Ni-doped MgH_2 give two reasons why we expect the dehydrogenation properties of the Ni doped MgH_2 to improve: (i) the weakened bonding between the Mg1 and H1 or Mg2 and H2 atoms as indicated by the reduced bonding peaks in the energy range from −7.5 to −3.5 eV and (ii) the higher probability of forming second phase Mg_2NiH_4 as implied by both the geometric features (the structural similarity between the NiH_4 groups in the present system and the Mg_2NiH_4 phase) and the characteristics of the partial DOS (the slight overlaps between the Ni d states and the Mg s and p states in the energy region from −1.4 eV to the Fermi energy in Figure 5b). Similar effects were observed in the Ni bulk doped MgH_2.[9]

3.3. Dehydrogenation Energy. We calculated the dehydrogenation energy of hydrogen atom from the (110) surface of MgH_2 using the formula below to further clarify the effects of the dopants on the dehydrogenation properties of MgH_2

$$E_d = \left[E(Mg_{32-x}M_{x+y}H_{63}) + \frac{1}{2}E(H_2)\right] - E(Mg_{32-x}M_{x+y}H_{64}) \quad (2)$$

The energy of the H dehydrogenated system $E(Mg_{32-x}M_{x+y}H_{63})$ was estimated using the final structure of the $Mg_{32-x}M_{x+y}H_{64}$ system after removing the H1 atom, but keeping the geometry of the supercell and the coordinates of remaining atoms unchanged. The energy of a hydrogen molecule, $E(H_2)$, was calculated as −6.773 eV using a 1 × 1 × 1 nm supercell. Values of E_d are listed in Table 1.

The E_d of the undoped MgH_2 ($x = 0$ and $y = 0$ in eq 2) is 1.92 eV. The E_d of the Al doped system slightly higher as predicted by the above analysis of the system's geometry (the reduction in the Mg−H1 bond length) and electronic structures (the overlap between the Mg1 p and the H1 s states at −3.1 eV below the Fermi energy). This means Al only has a small influence on the surface structure and the electronic structure, and so the dehydrogenation properties of MgH_2.

In the Ti-doped systems, the values of E_d are 1.69 and 1.61 eV for substitutional and interstitial occupation. The analysis above shows that Ti occupies the interstitial site with lower occupation energy. In the Ti interstitially doped system, Ti can distort the atoms in its vicinity and the sp hybridization between it and the two H2 atoms means it can capture them to form the TiH_2 phase (Figure 3). Both the formation of TiH_2 and the distortion will improve the dehydrogenation properties of the doped MgH_2. Experimental results show that ball milling the MgH_2 with TiH_2 can dramatically reduce the onset temperature and activation energy of the MgH_2 dehydrogenation reaction.[35]

Although the Mn substitution system had a lower dehydrogenation energy than the Mn interstitial occupation system it had a higher occupation energy, implying that this system is unlikely to occur in practice. The energy needed to dehydrogenate hydrogen in the Mn interstitial occupation system is 1.51 eV, about 21% lower than that of undoped MgH_2. As Figure 4, panels a and b, shows, the H1 and H2 atoms have been freed in this system and only weakly interact with the Mn atom as there are no overlaps between these atoms in the DOSs of this system. The combination of these effects improves the dehydrogenation properties of MgH_2.

As in the Mn-doped system, the Ni substitution system had a lower dehydrogenation energy and a higher occupation energy than the Ni interstitial occupation system. The occupation energy of the Ni interstitial occupation system was the lowest of all the considered systems. The reduction in the dehydrogenation energy of the Ni-doped system clearly indicates that Ni improves the dehydrogenation properties of MgH_2.

4. Conclusions

This paper uses first principles calculations to study the (110) surface of Al, Ti, Mn, and Ni doped MgH_2 systems. It shows that the Al prefers to substitute for a Mg atom, while Ti, Mn, and Ni prefer to occupy an interstitial site. These dopants use different mechanisms to improve the dehydrogenation properties of MgH_2. Adding Al causes the Mg2−H2 bond to stretch but compresses the Mg1−H1 bond outside the surface, which marginally increases the dehydrogenation energy. The DOSs of this system indicate a weak improvement of the dehydrogenation properties. This means that it is easier to break the Mg−H bonds, especially the Mg2−H2 bonds, in this system than in its undoped counterpart. The Ti, Mn, and Ni prefer to occupy an interstitial site that has a low occupation energy. The H atoms in the vicinity of the dopant of the Ti-doped system were dramatically distorted. The two H atoms attracted by the Ti could be used to generate TiH_2 phase and another H atom was freed from its host Mg atom, reducing the dehydrogenation energy. A Mn−H cluster with a similar structure to that in Mg_3MnH_7 was formed in the Mn doped system, but interactions between the Mn and H atoms are weak as the partial DOSs of this system show that the Mn d and H s states do not overlap. The distortion of the surface and the weak interactions between the atoms in this system improve the dehydrogenation properties of the Mn-doped MgH_2. A regular tetrahedral NiH_4 group structurally very similar to the group in Mg_2NiH_4 was formed in the Ni-doped MgH_2. Doping the MgH_2 with Ni should improve its dehydrogenation properties because (i) the bonding between the Mg and H atoms is weakened and (ii) there is a higher probability of forming the thermodynamically less stable Mg_2NiH_4 phase.

Acknowledgment. This work was supported by the National Basic Research Programme of China Grant 2006CB605104, the Natural Science Foundation of Shandong, China (Y2007F61) and the Programme of the Excellent Team of Harbin Institute of Technology.

References and Notes

(1) U.S. Department of Energy, Multi-Year Research, Development and Demonstration Plan: Planned program activities for 2004−2015, http://www1.eere.energy.gov/hydrogenandfuelcells/mypp/.
(2) Bogdanovic, B.; Hartwig, H. T.; Spliethoff, B. *Int. J. Hydrogen Energy* **1993**, *18*, 575.
(3) Liang, G.; Huot, J.; Boily, S.; van Neste, A.; Schultz, R. *J. Alloys Compd.* **1999**, *292*, 247.
(4) Hanada, N.; Ichikawa, T.; Fujii, H. *J. Phys. Chem. B* **2005**, *109*, 7188.
(5) Song, M. Y.; Bobet, L. J.; Darriet, B. *J. Alloys Compd.* **2002**, *340*, 256.
(6) Barkhordarian, G.; Klassen, T.; Bormann, R. *Scripta Mater.* **2003**, *49*, 213.
(7) Polanski, M.; Bystrzycki, J.; Plocinski, T. *Int. J. Hydrogen Energy* **2008**, *33*, 1859.
(8) Song, Y.; Guo, Z. X.; Yang, R. *Mat. Sci. Eng. A* **2004**, *365*, 73.
(9) Song, Y.; Guo, Z. X.; Yang, R. *Phys. Rev. B* **2004**, *69*, 094205.
(10) Shang, C. X.; Bououdina, M.; Song, Y.; Guo, Z. X. *Int. J. Hydrogen Energy* **2004**, *29*, 73.
(11) Bogdanović, B.; Hofmann, H.; Neuy, A.; Reiser, A.; Schlichte, K.; Spliethoff, B.; Wesse, S. *J. Alloys. Compd.* **1999**, *292*, 57.
(12) Bobet, J. L.; Even, C.; Nakamura, Y.; Akiba, E.; Darriet, B. *J. Alloys, Compd.* **2000**, *298*, 279.
(13) Gutfleisch, O.; Dal Toè, S.; Herrich, M.; Handstein, A.; Pratt, A. *J. Alloys Compd.* **2005**, *404−406*, 413.
(14) Jensena, T. R.; Andreasen, A.; Vegge, T.; Andreasen, J. W.; Ståhl, K.; Pedersenb, S. A.; Nielsenf, M. M.; Molenbroekg, A. M.; Besenbacher, F. *Int. J. Hydrogen Energy* **2006**, *31*, 2052.
(15) Lu, H. B.; Poha, C. K.; Zhang, L. C.; Guo, Z. P.; Yu, X. B.; Liu, H. K. *J. Alloys Compd.* **2009**, *481*, 152.
(16) Zaluska, A.; Zaluski, L.; Ström-Olsen, J. O. *J. Alloys Compd.* **1999**, *288*, 217.
(17) Lu, J.; Choi, Y J.; Fang, Z Z.; Sohn, H Y.; Rönnebro, E. *J. Am. Chem. Soc.* **2009**, *131*, 15843.
(18) Larsson, P.; Araújo, C. M.; Lasson, J. A.; Jena, P.; Ahuja, R. *Proc. Natl. Acad. Sci.* **2008**, *105*, 8227.
(19) Liang, J. J. *J. Alloys Compd.* **2007**, *446−447*, 72.
(20) Song, Y.; Zhang, W. C.; Yang, R. *Int. J. Hydrogen Energy* **2009**, *34*, 1389.
(21) Pozzo, M.; Alfè, D. *Int. J. Hydrogen Energy* **2009**, *34*, 1922.
(22) Kelkar, T.; Pal, S. *J. Mater. Chem.* **2009**, *19*, 4348.
(23) Li, S.; Jena, P.; Ahuja, R. *Phys. Rev. B* **2006**, *74*, 132106.
(24) Du, A. J.; Smith, S. C.; Yao, X. D.; Lu, G. Q. *Surf. Sci.* **2006**, *600*, 1854.
(25) Kresse, G.; Hafner, J. *Phys. Rev. B* **1993**, *47*, 558.
(26) Kresse, G.; Furthmüller, J. *Phys. Rev. B* **1996**, *54*, 11169.
(27) Perdew, J. P.; Chevary, J. A.; Vosko, S. H.; Jackson, K. A.; Pederson, M. R.; Singh, D. J.; Fiolhais, C. *Phys. Rev. B* **1992**, *46*, 6671.
(28) Kresse, G.; Joubert, D. *Phys. Rev. B* **1999**, *59*, 1758.
(29) Bortz, M.; Bertheville, B.; Böttger, G.; Yvon, K. J. *J. Alloys Compd.* **1999**, *287*, L4.
(30) Song, Y.; Dai, J. H.; Li, C. G.; Yang, R. *J. Phys. Chem. C* **2009**, *113*, 10215.
(31) Song, Y.; Dai, J. H.; Liang, X. M.; Yang, R. *Phys. Chem. Chem. Phys.* **2009**, under review.
(32) van Setten, M. J.; Brocks, S.; Er, G.; de Groot, R. A.; de Wijs, G. A. *Phys. Rev. B* **2009**, *79*, 125117.
(33) Tiwari, S.; Er, D.; de Wijs, G. A.; Brocks, G. *Phys. Rev. B* **2009**, *79*, 024105.
(34) Bortz, M.; Bertheville, B.; Yvon, K.; Movlaev, E. A.; Verbetsky, V. N.; Fauth, F. *J. Alloys Compd.* **1998**, *279*, L8.
(35) Choi, Y. J.; Lu, J.; Sohn, H. Y.; Fang, Z. Z.; Rönnebro, E. *J. Phys. Chem. C* **2009**, *113*, 19344.

JP103066G